Journal of Industrial and Engineering Chemistry 82 (2020) 89–97

Contents lists available at ScienceDirect

Journal of Industrial and Engineering Chemistry

journal homepage: www.elsevier.com/locate/jiec

Injectable thermoresponsive hydrogel/nanofiber hybrid scaffolds inducing human adipose-derived stem cell chemotaxis

Youngjoo Choi[a], Min Hee Park[b,*], Kangwon Lee[a,*]

[a] Department of Transdisciplinary Studies, Graduate School of Convergence Science and Technology, Seoul National University, Seoul 08826, Republic of Korea
[b] Center for Convergence Bioceramic Materials, Korea Institute of Ceramic Engineering and Technology, Cheongju 28160, Republic of Korea

ARTICLE INFO

Article history:
Received 17 August 2019
Received in revised form 24 September 2019
Accepted 26 September 2019
Available online 5 October 2019

Keywords:
Injectable hydrogel
Thermoresponsive hydrogel
Cell recruitment
Adipose-derived stem cells
Biomaterials
Drug releasing

ABSTRACT

Hydrogels with three-dimensional networks similar to extracellular matrix (ECM) have been widely investigated as biomaterials in tissue engineering. Injectable hydrogels have been studied for less invasive treatments, and moreover, the endogenous cell recruitment capability can create synergy with these hydrogels for repairing damaged tissues. However, their low mechanical properties or difficult process has been a disadvantage for their use in load-bearing cartilage such as intervertebral disc. Therefore, high-modulus injectable hydrogels which have the potential in cell recruitment are required for fundamental and less invasive treatments. In this study, we fabricated injectable and thermoresponsive hybrid scaffolds comprising chitosan/gelatin hydrogel and polycaprolactone nanofibers, and we added platelet-derived growth factor-BB (PDGF-BB) within the hybrid scaffolds to recruit human adipose-derived stem cells (hADSCs). The modulus of the hybrid scaffolds was approximately 0.9 MPa after gelation at 37 °C with structural similarity to the ECM. Also the modulus could be managed by changing the concentration of the components in the hybrid scaffolds. The release of PDGF-BB from the hybrid scaffolds induced hADSC chemotaxis under rough condition which chemoattractant was diluted by serum free cell culture medium. Our proposed hybrid scaffolds are promising candidates for less invasive tissue engineering strategies to induce endogenous hADSC recruitment.

Introduction

Hydrogels have been widely used in tissue engineering as matrixes and molecular carriers. Among the various polymers, hydrogels offer advantages such as three-dimensionally cross-linked networks consisting of hydrophilic chains, and therefore, exhibit high water content and a similar structure to the extracellular matrix (ECM) [1]. As various application of hydrogels, there are solid molded form, particles, membranes, or injectable therapeutic method [2]. Injection method can be applied to a less invasive implant treatment. The method has advantages of forming any defective site and desired shape [3]. Also the porosity of injectable hydrogels enables cells to migrate and proliferate [1]. Despite the benefits of injectable hydrogels, low mechanical properties are major disadvantages, and it need difficult process to improve mechanical properties. However, their low mechanical properties or difficult process has been a limitation for their use in load-bearing cartilage such as intervertebral disc (IVD). Therefore, simply fabricated injectable hydrogels with high modulus should be investigated for less invasive treatments for load-bearing cartilage.

Chitosan hydrogel, a suitable candidate as the injectable hydrogel, has thermoresponsive characteristic which is fluidic state at low temperature and gelates at higher temperature as body temperature. It exhibits higher modulus when is gel at high temperature and is injectable under fluidic phase at low temperature [4–6]. However, the modulus of chitosan hydrogel is still insufficient to support high pressure of load-bearing cartilage tissues and blending can be one of the strategies to improve modulus of hydrogels [7]. Modulus of hydrogels is enhanced by blending other polymers such as gelatin. Gelatin is obtained from thermo-treated collagen, which promote cell adhesion and proliferation via its Arg-Gly-Asp like sequence in the protein [8]. When chitosan and gelatin are blended, linear cationic polysaccharide chitosan and negatively charged gelatin form polyelectrolytic complexes in acidic aqueous solution. Hydrogen bond between chitosan and gelatin increases by neutralizing pH [9,10]. In biological aspect, composites of chitosan/gelatin have structural similarity to glycosaminoglycans and collagen. Since

* Corresponding authors.
E-mail addresses: minheepark@kicet.re.kr (M.H. Park), kangwonlee@snu.ac.kr (K. Lee).

https://doi.org/10.1016/j.jiec.2019.09.046
1226-086X/

these components comprise the ECM, chitosan/gelatin hydrogel forms compatible environment for cells [9]. Furthermore, electrospun polycaprolactone (PCL) nanofibers which are generally used as biomaterials have high elasticity and structural similarity to the ECM in the cartilage, and thus blending PCL nanofibers in other matrix may result in a promising structure and enhanced modulus for tissue engineering applications of load-bearing cartilage [11–13]. Although materials of the scaffolds (chitosan, gelatin, and PCL) have been widely used as biomaterials, this can be positive because there are many research results using the materials, which demonstrate high potential and competitiveness in terms of clinical trials and cost [14,15].

Furthermore, in biological perspective, cell homing strategy which has been studied in tissue engineering has the potential for fundamental repair of damaged tissues. This strategy can overcome limitations of mosaicplasty or chondrocyte implantation treatments because it can induce endogenous tissue regeneration and is safe from the cell-based immune response and engraftment problems [16–20]. For the cell homing strategy, adipose-derived stem cell (ADSC) is appropriate cell to recruit for cartilage tissue regeneration because adipose tissue is plentiful in the human body and exists around various cartilage tissues [21]. In addition, stem cell derived from adipose tissue have capability of differentiating into other lineages such as chondrocyte [22–24]. ADSCs are recruited by cytokines or growth factors including platelet-derived growth factor–BB (PDGF-BB) [25,26]. Platelet-derived growth factor (PDGF) is a major mitogen in serum, which regulates cell migration, proliferation, and angiogenesis [27]. Especially PDGF-BB is chemoattractant exhibiting a more effective ADSC recruitment among the PDGF family because the activation of the PDGF receptor β affects ADSC migration [28,29].

In this study, we developed three-dimensional hybrid scaffolds comprising chitosan/gelatin hydrogel and PCL nanofibers to induce chemotaxis of human adipose-derived stem cell (hADSC). We hypothesized that the addition of PCL nanofibers mimics not only the microenvironment of the ECM but also enhances the modulus of hybrid scaffolds, and the final hybrid scaffolds containing PDGF-BB can successfully recruit hADSCs. After fabricating the hybrid scaffolds containing PDGF-BB, we investigated the dynamic mechanical properties, PDGF-BB release profile, and various biological activities of the cells, such as cytotoxicity and chemotaxis (Scheme 1).

Experimental

Materials

Chitosan (low molecular weight, deacetylated chitin), gelatin (from porcine skin, gel strength 300, Type A), and polycaprolactone (PCL, Mn: 80,000), sodium bicarbonate ($NaHCO_3$, BioReagent), 2,2,2-trifluoroethanol (2,2,2-TFE), 4′,6-diamidino-2-phenylindole (DAPI), and Sigmacote® were obtained from Sigma-Aldrich (St Louis, MO, USA). Hydrochloric acid (HCl, 35.0–37.0%) and sodium hydroxide (NaOH, bead, 98.0%) were purchased from Samchun (Gyeonggi-do, Korea). Paraformaldehyde (4%, molecular biology applications) was purchased from Biosesang (Gyeonggi-do, Korea). Platelet-derived growth factor-BB (PDGF-BB, recombinant human (*Escherichia coli*-derived), Carrier Free) was purchased from R&D Systems (Minneapolis, MN, USA). Human PDGF-BB ELISA kit was obtained from Abcam (Cambridge, UK). Human adipose-derived stem cells (hADSCs) were obtained from Cefobio (Seoul, Korea). Cell Counting Kit-8 (CCK-8) was obtained from Dojindo Laboratories (Tokyo, Japan). LIVE/DEAD™ Viability/Cytotoxicity Kit was obtained from ThermoFisher (Waltham, MA, USA). Foetal bovine serum (FBS) was purchased from CellSera (Rutherford, NSW, Australia).

Preparation of hybrid scaffolds

Hybrid scaffolds

Chitosan hydrogel solution was produced by dissolving 0.2 g of chitosan in 10 mL of a 0.1 M hydrochloric acid aqueous solution to form 2% w/v hydrogel, and stirring overnight in a 4 °C ice bath. Gelatin solutions of various concentrations were prepared by dissolving gelatin in deionized water (DW) at 40 °C for 3 h. After the chitosan and gelatin solutions were separately fabricated, 1 mL of each gelatin solution was dropped into the chitosan solution in a 4 °C ice bath under stirring for 15 min to obtain a homogeneous mixture. Then to adjust to neutral pH, 1 mL of cooled 1.0 M sodium bicarbonate aqueous solution was dropped into the chitosan/gelatin hydrogel solution under stirring in an ice bath. The obtained hydrogel solution was stirred for 30 min to obtain a homogeneous mixture. Thus, chitosan/gelatin hydrogel solution was allowed to gelate at 37 °C.

The PCL nanofibers were fabricated as follows by the electrospinning method. The PCL solution was produced by dissolving PCL in 2,2,2-TFE to form a 15% w/v solution. For electrospinning, a positive voltage of 15 kV was allowed to the solution through a 25 G metal needle at a constant feeding rate (0.7 mL h^{-1}). The length between the collecting plate and the needle was maintained at 15 cm. The electrospun PCL nanofibers were collected directly on a clean aluminum foil placed on the collecting plate. The PCL nanofibers on the foil were detached by spraying DW and hydrolyzed in a 1 M sodium hydroxide solution for 8 h, followed by washing thrice with DW to remove the residuary salts and drying at room temperature. The dried PCL nanofibers were cut into 1 mm squares and then ripped using tweezers. The cut and

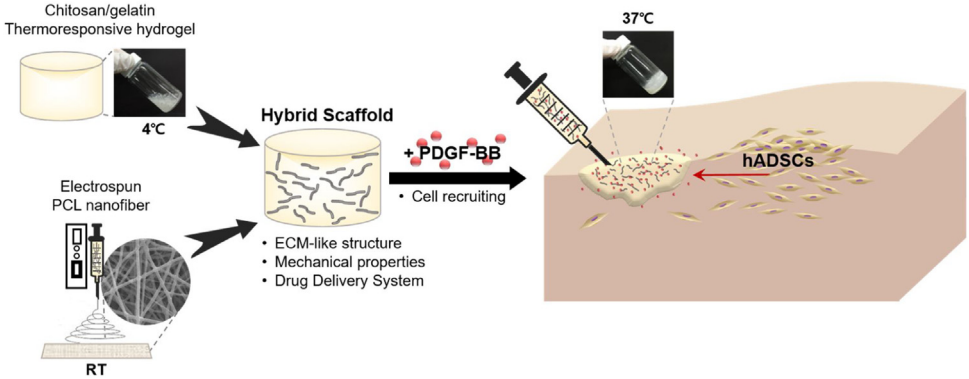

Scheme 1. Schematic illustration of the chitosan/gelatin hydrogel-based PCL nanofiber hybrid scaffolds preparation for hADSC chemotaxis. After the injection of the hybrid scaffolds, a subsequent increase in the temperature to 37 °C induces their gelation, followed by the release of the embedded PDGF-BB.

ripped PCL nanofibers were added to 10 mL of chitosan/gelatin hydrogel solution in a 4 °C ice bath and stirred to obtain a homogeneous fluidic hybrid scaffold, which was then gelated at 37 °C.

Hybrid scaffolds embedded with PDGF-BB

Hybrid scaffolds embedded with PDGF-BB were fabricated for recruiting the hADSCs. The PDGF-BB was reconstituted at 100 μg/mL in sterile 4 mM hydrochloric acid. Then, various amounts of PDGF-BB were added to a small amount of pre-gelled fluidic hybrid scaffolds and dispersed by pipetting. The hybrid scaffolds containing PDGF-BB formed a gel at 37 °C in response to the temperature.

Dynamic mechanical properties examination

The storage modulus (G′), loss modulus (G″), and tan (δ) of the chitosan/gelatin hydrogel and hybrid scaffold were investigated by the advanced rheometric expansion system (ARES, Rheometric Scientific, UK) as a function of temperature. The temperature of the ARES was set at 4 °C before investigation. The samples, which were in a fluidic state at 4 °C, were loaded between the parallel plates of 8.0 mm diameter. After the samples were loaded, the temperature was maintained at 4 °C for 10 min and raised to 37 °C at a heating rate of 2 °C min^{-1} and then maintained at 37 °C for 20 min. The experiment proceeded under a controlled frequency (1.0 rad s^{-1}) and 5% strain.

Inverted tube test

To confirm the gelation of the chitosan/gelatin hydrogels and hybrid scaffolds, an inverted tube test was performed. 2 mL of the chitosan/gelatin hydrogel or hybrid scaffold samples, which were at 4 °C, were injected into 10 mL glass vials, which were then placed in a 37 °C water bath for 10 min. Gelation was confirmed when the glass vials were tilted and the samples were not fluidic.

Fourier transform infrared (FTIR) spectrometer

The hybrid scaffolds were chemically characterized using a Fourier transform infrared (FTIR) spectrometer (ALPHA, Bruker, MA, USA). The FTIR spectra of chitosan, gelatin, PCL nanofibers, and the dried hybrid scaffolds, which was chitosan/gelatin hydrogel with PCL nanofibers, were recorded within a frequency range 4000–400 cm^{-1} at room temperature.

Scanning electron microscopy (SEM)

The morphologies of the chitosan/gelatin hydrogel and PCL nanofibers and hybrid scaffolds were observed using Scanning electron microscopy (SEM) (SNE-4500 M, NanoImages, CA, USA). The fluidic polymer solution of chitosan/gelatin hydrogel and hybrid scaffolds, which had been at 4 °C, was injected into the glass vials and placed in a 37 °C water bath for gelation. Then, the samples were quenched in liquid nitrogen at −196 °C before subsequent freeze drying. The electrospun PCL nanofibers were collected on a clean aluminum foil and dried at room temperature. The foil with the collected PCL nanofibers was then cut into 1 cm squares to obtain intact PCL nanofibers and hydrolyzed PCL nanofibers were cut into 1 cm squares after at room temperature. All samples were sputter-coated (MCM-100, Sec, Gyeonggi-do, Korea) with platinum before performing SEM.

In vitro cytotoxicity assay

The cytotoxicity assay was performed using both direct and indirect contact method. The direct contact method was performed by seeding the cells onto the gelated hybrid scaffolds and indirect contact method was achieved by following ISO 10993-12 [30]. According to ISO 10993-12, the extracts were produced by steeping the gelated hybrid scaffolds in Dulbecco's modified Eagle's medium (DMEM) at an extraction ratio of 6 cm^2 mL^{-1} for 24 h at 37 °C in an incubator. The extracts were diluted with DMEM at various ratios: volumes of 100%, 50%, 25%, and 12.5% extracts in DMEM. The cells were treated with each diluted extract and the control groups were treated using 0% extracts in DMEM.

Cell culture

Human adipose-derived stem cells (hADSCs) (passage 5) were used for the in vitro assay. The hADSCs were cultured in high-glucose DMEM and 10% FBS with 1% penicillin-streptomycin (PS), followed by incubation at 37 °C under a humidified 5% CO_2 conditioned atmosphere. The medium in which the hADSCs were cultured was changed every 2–3 days.

Cell viability assay

Before the experiment, the hADSCs were cultured onto 96-well plates with 5×10^3 cells per well for 24 h. Next, the medium that remained on the 96-well plates was suctioned and the cells were treated with the diluted extracts and control medium for 1, 4, and 7 days in a humidified 37 °C incubator under a 5% CO_2 atmosphere. Then, the cell viability at each time point (1, 4, and 7 days) was examined by a CCK-8. The CCK-8 work solution was added to each well and incubated for 2 h at 37 °C, which was followed by the recording of the optical density (OD) of the wells at 450 nm using a microplate reader (Synergy H1, BioTek, VT, USA).

Live/dead assay

For the direct contact method, the hybrid scaffolds were loaded in a 96-well plates with 30 μL per well and gelated before seeding cells, and then the hADSCs were seeded onto the hybrid scaffolds with 5×10^3 per well. These hADSCs seeded scaffolds were cultured for 7 days in high-glucose DMEM and 10% FBS with 1% PS, followed by incubation at 37 °C under a humidified 5% CO_2 conditioned atmosphere. For the indirect contact method, the hADSCs were cultured onto 24-well plates with 3×10^4 cells per well 24 h before the experiment. Next, the medium that remained on the 96-well plates was suctioned and the cells were treated with the diluted extracts and control medium for 1, 4, and 7 days in a humidified 37 °C incubator under a 5% CO_2 atmosphere. Then, the cell viability at each time point (i.e., day 1, 4, and 7) was observed by a LIVE/DEAD™ Viability/Cytotoxicity Kit. The hADSCs and the scaffolds were treated with a working solution including ethidium homodimer-1 and calcein AM for 45 min in the dark at room temperature. The hADSCs and the scaffolds were washed with Dulbecco's phosphate-buffered saline (DPBS) twice and observed by a fluorescence microscope (Azio Observer Z1, Carl Zeiss, Oberkochen, Germany).

PDGF-BB release from hybrid scaffolds

As the PDGF-BB was released from the hybrid scaffolds, the release kinetics were investigated by enzyme-linked immunosorbent assay (ELISA). To assess the PDGF-BB release from the hybrid scaffolds, Sigmacote® coated 20 mL glass vials were prepared for inhibiting undesired growth factor attachment on the glass during the releasing experiment. The glass vials were coated by swirling the Sigmacote® over the vials and air-dried for 10 h. The vials were then rinsed thrice with sterile DW and air-dried. Then, 1 mL of gelated hybrid scaffolds including various amounts of PDGF-BB were loaded in the Sigmacote® coated glass vials and 5 mL of phosphate-buffered saline (PBS) (pH 7.4) was poured, which was used as the releasing medium. Various amounts of PDGF-BB, 1000,

500, and 100 ng, per 1 mL of hybrid scaffolds were used to prepare the samples, which were then placed in a 37 °C water bath. At the predetermined time points, 500 μL of the PBS solution was gathered and stored at −20 °C for later use, and replaced with 500 μL of pure PBS. The release profile of the PDGF-BB was analyzed by the human PDGF-BB ELISA kit (Abcam) following the manufacturer's instructions. Cumulative release over 21 days was performed on all samples. The experiment was conducted in triplicate for each condition and the data for each point was determined as the average of the experiments.

Examination of hADSC chemotaxis

To examine the hADSC chemotaxis, a stringent migration assay was performed on the cell culture dish. The stringent migration assay is a revised cell migration assay to mainly examine the chemotaxis rather than the chemokinesis [31,32]. To confirm the efficiency of the hADSC chemotaxis of the PDGF-BB released from the hybrid scaffolds, 60 × 15 mm circular cell culture dishes with straight lines drawn outside of under dishes were prepared and the hADSCs (passage 5) were cultured in the dishes at 8×10^5 cells per dish until the cell was grown to confluence in the DMEM cell culture medium. The hADSCs beyond the drawn line in the dishes were scrapped by a cell scraper to match the front line of the cells and drawn line outside the dish. Subsequently, 1 mL of the gelated hybrid scaffolds, including various amounts of PDGF-BB were located on the cell-free side of the dishes, 2 cm apart from the remaining hADSCs. The hybrid scaffolds containing various amounts of PDGF-BB (1000, 500, and 100 ng per 1 mL of hybrid scaffolds) and PDGF-BB-free hybrid scaffolds for control were prepared. The basic DMEM without any serum was used for the experiment to observe cell migration with minimum effect of cell proliferation. The sample dishes were incubated in a humidified 37 °C incubator under 5% CO_2 atmosphere for 48 h for inducing hADSC chemotaxis via hybrid scaffolds, releasing PDGF-BB under conditions similar to in vivo. After 48 h of culture, the hybrid scaffolds were removed and the hADSCs were fixed by 3 mL of 4% paraformaldehyde solution for 10 min and stained with DAPI for 30 min to identify the hADSC chemotaxis. The hADSCs that migrated across the drawn line were examined under a fluorescence microscope. To quantify the location and number of migrated hADSCs, ImageJ software were used.

Statistical analysis

All data are represented as the mean ± standard deviation. Analysis of variance (ANOVA) was performed for statistical evaluation. When the p-value was less than 0.05, it was regarded statistically significant. In the figures, the * and ** indicate $p < 0.05$ and $p < 0.01$ respectively.

Results and discussion

Fabrication and characterization of hybrid scaffolds

The hybrid scaffolds were constructed using porous chitosan/gelatin hydrogel and electrospun PCL nanofibers. The chitosan/gelatin hydrogel was prepared by blending the chitosan and gelatin solutions and neutralizing pH. The chitosan/gelatin hydrogel was a clear light yellow at 4 °C, in a fluidic aqueous phase, and turned opaque when gelated at 37 °C. When 2 mL of the chitosan/gelatin hydrogel was loaded in a 10 mL glass vial, sol to gel transformation took an average of 8.5 min at 37 °C. The structure of the chitosan/gelatin hydrogels exhibited highly porous morphology with composed of various gelatin concentrations. The pore size was decreased with increasing gelatin concentration in the hydrogel (Fig. S1). Among the various pore size of different hydrogels, the hydrogel with large pore was preferred because it can allow cells to migrate into the scaffolds after recruiting. And the difference in gelatin ratio in the hybrid scaffolds does not show a significant increase in modulus of scaffolds at 37 °C (Fig. 2c). Accordingly, the hybrid scaffolds were experienced with 1% gelatin concentration which showed the largest pore size (36.87 ± 2.68 μm) among all hydrogel samples. Since the hADSC has an average size of 20–30 μm [33,34], the chosen hydrogel was proper as a purposed scaffold.

In order to mimic the structure of native ECM and enhance the modulus of the hydrogels, we added PCL nanofibers after fabricating chitosan/gelatin hydrogel. Many studies have attempted to mimic native ECM structure for better cell proliferation and metabolism in the scaffolds [1,35,36]. The collagen fibers within the ECM of the human body have a diameter of submicron to a few μm [37,38]. Therefore, we manufactured PCL nanofibers exhibiting a uniform and repeatable average diameter of approximately 1 μm under the electrospinning condition at 15% w/v PCL and 15 kV. The electrospun PCL nanofibers were hydrolyzed using sodium hydroxide to be ripped and then blended with chitosan/gelatin hydrogel. The produced electrospun PCL nanofibers become slightly thinner through hydrolysis (Fig. S3). Hydrolysis cleaves the ester bonds in the PCL, producing a nanoroughness and carboxylate functional group, and thus the resilience of the PCL nanofibers is reduced and the hydrophilicity of the PCL is increased [39,40].

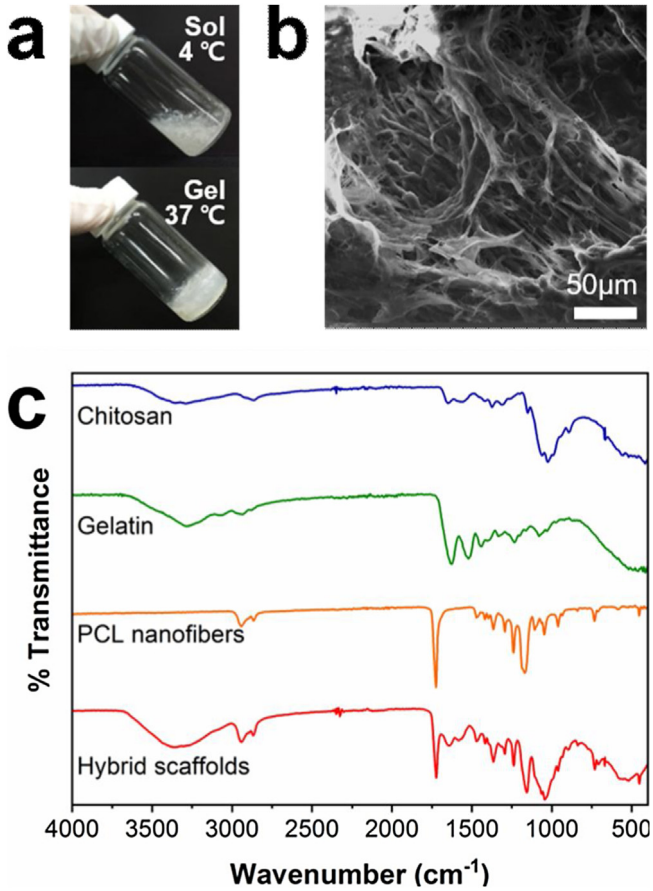

Fig. 1. Characterization of the hybrid scaffolds comprising 0.1% w/v gelatin (1 mL of 1% gelatin solution in 10 mL of hybrid scaffolds) and 1.5% w/v PCL nanofibers. (a) Images of thermoresponsive gelation behaviors of the hybrid scaffolds at 4 °C and 37 °C. (b) SEM image of the hybrid scaffolds. (c) FTIR spectra of chitosan, gelatin, PCL, and the hybrid scaffolds.

The hybrid scaffolds were successfully fabricated by blending the chitosan/gelatin hydrogel and electrospun PCL nanofibers. The hybrid scaffolds were fluidic at 4 °C and gelated at 37 °C, as they did not flow at 37 °C (Fig. 1a). The hybrid scaffolds comprising 0.1% w/v gelatin and 1.5% w/v PCL nanofibers in hydrogel were observed by SEM. Fig. 1b shows the morphological differences in the hybrid scaffolds compared with the chitosan/gelatin hydrogels without PCL nanofibers. We observe that the hybrid scaffolds exhibit a structure similar to the native ECM. Furthermore, the FTIR spectra of chitosan, gelatin, hydrolyzed PCL nanofibers, and hybrid scaffolds are shown in Fig. 1c. The FTIR spectrum of chitosan shows broad peaks at 3450 cm^{-1} corresponding to the stretching of the N—H and O—H bonds, while the peaks at 1646, 1561, and 1028 cm^{-1} are the peaks of amide I, amide II, and C–O stretching vibrations (–C—O—C–), respectively. The FTIR spectrum of gelatin shows peaks at 3282 cm^{-1} for N—H stretching, 1628 cm^{-1} for C=O stretching, and 1520 cm^{-1} for the N—H bending of amide II. PCL absorbs at 2940 cm^{-1}, 1726 cm^{-1}, and 1167 cm^{-1} due to C–H stretching, C=O stretching, and C—O—C stretching vibrations, respectively. The hybrid scaffold maintains the characteristic peaks of chitosan, gelatin, and PCL, besides the slight peak shifts caused by the blending components.

Dynamic mechanical properties of hydrogel and hybrid scaffolds

The dynamic mechanical properties were assessed by ARES and the values of the storage modulus (G′), loss modulus (G″), and tan (δ) were measured at the increasing temperature from 4 °C to 37 °C. The chitosan/gelatin hydrogel and hybrid scaffold were in the fluidic aqueous phase at 4 °C and gelated at 37 °C in response to the thermal changes, resulting in considerably enhanced moduli. The storage modulus exhibited by the chitosan/gelatin hydrogel at 37 °C under all conditions was much higher than that at 4 °C, confirming its thermoresponsive properties (Fig. 2a). Among the conditions, there was no significant difference in the middle range of gelatin concentrations. However, for the 1%, 2.5%, and 5% gelatin concentrations (1 mL of each gelatin solution in 10 mL of chitosan hydrogel), the storage modulus increased with increasing gelatin concentration. After 10 min at 37 °C, the 1%, 2.5%, and 5% gelatin solutions included hydrogels exhibited an average G′ of 35.45 ± 0.5, 144.47 ± 0.8, and 383.8 ± 1 kPa, respectively.

The hybrid scaffolds comprising 0.1% w/v gelatin (1 mL of 1% gelatin solution in 10 mL of hybrid scaffolds) and 1.5% w/v PCL nanofibers are observed to exhibit the highest G′ of 0.883 ± 0.01 MPa at 37 °C after injection, which was about 10^4 times higher than that at 4 °C and demonstrated thermoresponsive properties (Fig. 2b). Meanwhile, the modulus of the gelated hybrid scaffolds at 37 °C varies with the ratio of the components. The final storage moduli of the hybrid scaffolds with various gelatin concentrations (1 mL of 1%, 1.5%, and 2% gelatin solution in 10 mL of hybrid scaffolds) and a fixed PCL ratio (1%) are similar (Fig. 2c). However, there is a notable difference in the modulus of each sample on increasing the PCL ratio in the hybrid scaffolds at a fixed gelatin ratio (1 mL of 1% gelatin solution in 10 mL of hybrid scaffolds) (Fig. 2d). The hybrid scaffolds composed of 0%, 1%, and 1.5% PCL exhibit a storage modulus of 37 ± 0.3 kPa, 109.43 ± 2 kPa, and 883.54 ± 1 kPa, respectively. We observe that the addition of the PCL nanofibers significantly increased the modulus of the hybrid scaffolds. However, despite the significant variation in the modulus for the different ratios of PCL, the structure of the hybrid scaffolds does not show any distinct differences (Fig. 2e). These results suggest that although the hybrid scaffolds have three-dimensional networks of chitosan/gelatin hydrogel, the nanofibers may strongly sustain the hybrid scaffolds. In addition, since PCL nanofibers support the hybrid scaffolds such as collagen fibers in the ECM, an increase of PCL concentration leads to a higher modulus after gelation of the hybrid scaffolds. Therefore, the modulus of the hybrid scaffolds can be controlled through the PCL concentration, while maintaining the injectable and thermoresponsive characteristics. Especially, the injectable hybrid scaffolds

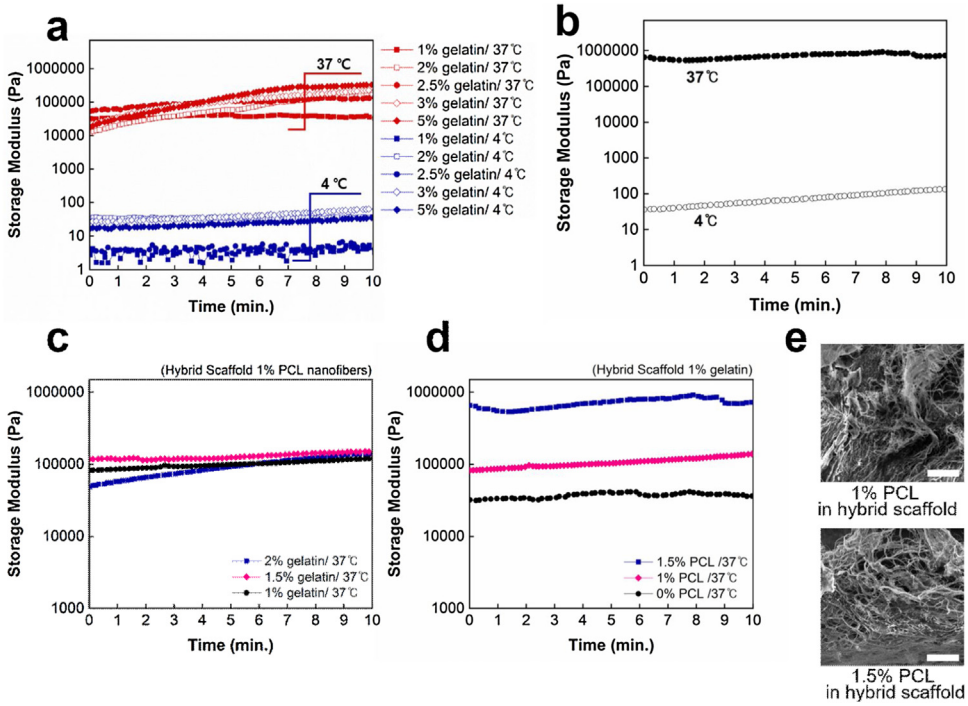

Fig. 2. Dynamic mechanical properties of chitosan/gelatin hydrogel and hybrid scaffolds at various concentrations and temperatures. (a) Difference of storage modulus in the chitosan/gelatin hydrogel in response to the temperature and gelatin concentration in the hydrogel. (b) Difference of storage modulus in the hybrid scaffolds in response to the temperature changes. (c) Difference of storage modulus in the hybrid scaffolds depending on various gelatin concentration. (d) Difference of storage modulus in the hybrid scaffolds depending on various PCL concentration. (e) SEM images of the hybrid scaffolds at different PCL concentrations (scale bar: 50 μm).

with 1.5% PCL exhibited a modulus close to 0.9 MPa after gelation, demonstrating that the hybrid scaffolds can effectively support themselves in the high pressure areas after injection and gelation at the desired site. In addition, modulus of the hybrid scaffolds is similar to that of native nucleus pulposus in the IVD (0.12–1 MPa) [41,42].

In vitro cytotoxicity assay

To assess the cytotoxicity of the hybrid scaffolds as biomaterials, the cell viability and proliferation of the hybrid scaffolds were assessed by CCK-8 and LIVE/DEAD™ Viability/Cytotoxicity Kit using the hADSCs, which were treated with the diluted hybrid scaffold extracts for 1, 4, and 7 days. The extracts were diluted with DMEM at various ratios: 100%, 50%, 25%, and 12.5% extract in DMEM. Fig. 3a shows the CCK-8 assay results of the hADSC viability after treatment with the diluted extracts for 1, 4, and 7 days. The viability of most groups was higher than 90%, or higher than that of the control group on day 1, 4, and 7. The results showed that even for the 100% extracts on day 7, the cell viability was approximately 80%. Fig. 3b shows the fluorescence images of the live (green) and dead (red) hADSCs after 1, 4, and 7 days of treatment with diluted extracts. The fluorescence images of the cells were achieved by the LIVE/DEAD™ Viability/Cytotoxicity Kit using a fluorescence microscope. The increase in the number of cells is observed to be analogous to the control group during the experiment days and dead cells were rarely observed in all diluted conditions on day 1, 4, and 7. Moreover, although the morphology of the hADSCs was slightly different compared with that of the control on day 4, the cell viability remained high. Fig. 3c shows the fluorescence images of the hADSCs directly seeded onto the hybrid scaffolds, and these scaffolds were cultured for 7 days. The live (green) and dead (red) hADSCs were also stained by the LIVE/DEAD™ Viability/Cytotoxicity Kit and observed using a fluorescence microscope on day 4 and 7. The number of live seeded cells were increased from day 4 to day 7, showing cell proliferation and high viability. Also the morphology of the hADSCs implies that the hADSCs could be penetrated into the hybrid scaffolds. Therefore, despite the minor variations in the results depending on the dilution rate of the extracts, the data indicate that the hybrid scaffolds are cytocompatible and suitable to applied in tissue engineering for use as tissue engineering scaffolds.

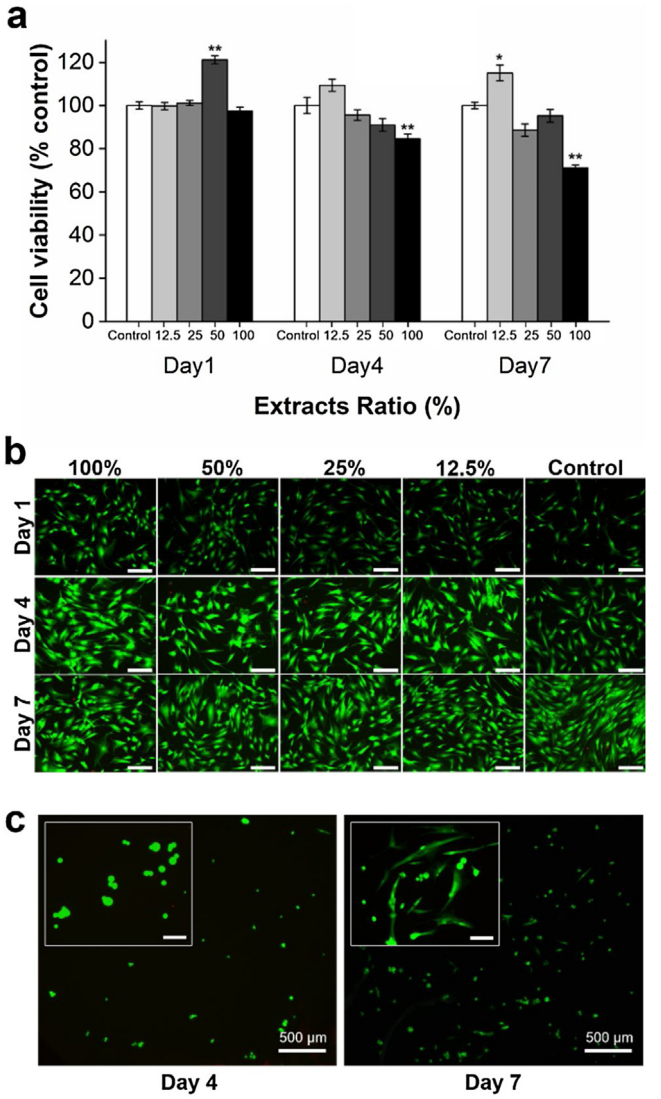

Fig. 3. Cytotoxicity assessment of the hybrid scaffolds. (a) Cell viability at each time point (1, 4, and 7 days) was examined by CCK-8. The hADSCs were treated with the hybrid scaffold eluate in a concentration-dependent manner for 1, 4, and 7 days. (b) Fluorescence images of the live (green) and dead (red) cells treated with the hybrid scaffold eluate at different ratios. The cytotoxicity of the hADSCs on day 1, 4, and 7 were observed (Scale bar: 200 μm). (c) Fluorescence images of the hADSCs seeded on the hybrid scaffolds. The live (green) and dead (red) cells were stained and observed on day 4 and 7. Enlarged inset images are show in the left (Scale bar of inset image: 100 μm). The asterisks (*) indicates statistically substantial differences compared with the control group (n = 7).

PDGF-BB release from hybrid scaffolds

PDGF-BB release and hADSC chemotaxis were investigated using our proposed hybrid scaffolds consisting of 0.1% gelatin and 1.5% of PCL, exhibiting a high storage modulus of approximately 0.9 MPa (0.883 ± 0.01 MPa). To examine the released PDGF-BB, the hybrid scaffolds containing various amounts of PDGF-BB were placed in PBS at 37 °C for 3 weeks. The assessment of the released PDGF-BB was made by ELISA. Cumulative release of PDGF-BB over time was analyzed by Boltzmann fitting of experimental data, and trend line was determined for each condition. The release property of PDGF-BB from the hybrid scaffolds is displayed in Fig. 4. The hydrogel scaffolds containing large amounts of PDGF-BB released larger amounts of PDGF-BB. Also the major release of PDGF-BB was found in the first 7 days in all groups. However, it shows a large loss in released PDGF-BB proportionately to the amount of loaded into

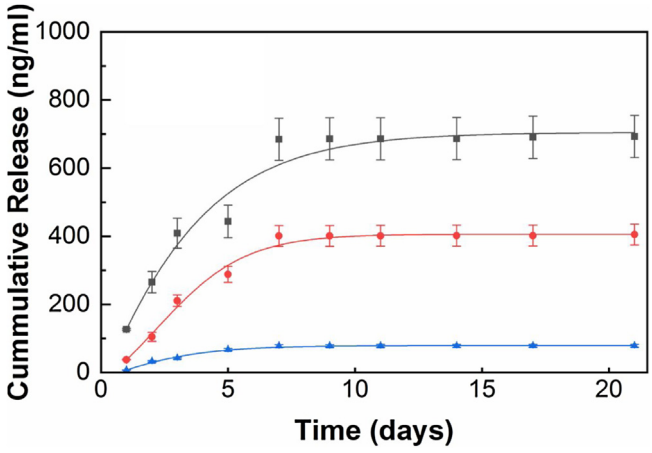

Fig. 4. Release property of the PDGF-BB from the hybrid scaffolds were determined by ELISA. The hybrid scaffolds embedded with PDGF-BB in PBS at 37 °C released PDGF-BB. Various amounts of PDGF-BB ((■) 1000 ng, (●) 500 ng, and (▲) 100 ng) were loaded in 1 mL of hybrid scaffolds. All the curves are analyzed by Boltzmann function. The R-squared value of all curves is greater than 0.99.

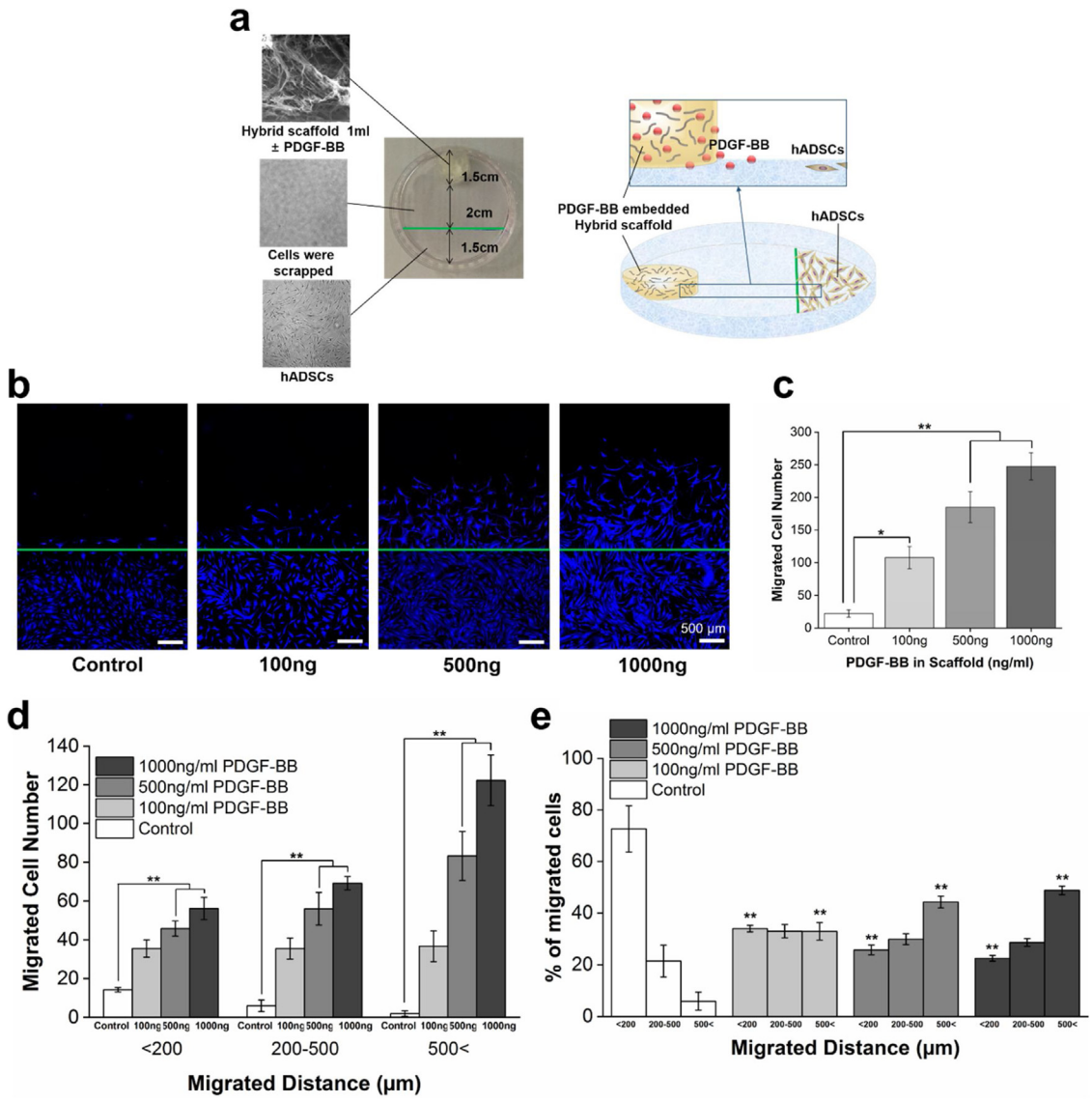

Fig. 5. Determination of hADSC chemotaxis induced by released PDGF-BB from hybrid scaffolds. A stringent migration assay was performed. (a) Schematic illustration showing the experimental preparation. The hADSCs were grown to confluence on the cell culture dishes and partly scrapped, followed by loading the gelated hybrid scaffolds containing PDGF-BB on the end point of the scrapped side on the dishes. The hybrid scaffolds contained various amounts of PDGF-BB (1000, 500, and 100 ng PDGF-BB per 1 mL of hybrid scaffold) and the control group did not contain PDGF-BB. The distance between the scaffolds and hADSCs was 2 cm. (b) After a 48 h incubation, DAPI stained hADSCs (blue) were examined by a fluorescence microscope. The images of the migrated hADSCs beyond the drawn line (green line) and confluent hADSCs inside the drawn line were identified (Scale bar: 500 μm). (c) Compared with the control group, a greater number of hADSCs are shown to migrate as the concentration of PDGF-BB in the hybrid scaffolds increases. (d) hADSCs migrate further toward the hybrid scaffolds with increasing concentration of PDGF-BB. (e) The distribution of the migrated cells according to the PDGF-BB concentration in the hybrid scaffolds. The greater the concentration of PDGF-BB, the higher the proportion of hADSCs that migrate beyond 500 μm. In the control group, the greatest percentage of hADSC migration is observed at a distance less than 200 μm. The asterisks (*) indicates statistically substantial differences compared with the control group. Three independent experiments were performed for each condition.

the scaffolds. The loss could be occurred when the same volume of hybrid scaffolds with different mass of PDGF-BB were transferred to other vials for releasing after gelation. During the 3 weeks, a small but sustained release was observed in the samples with 1000 ng of PDGF-BB during the 3 weeks while the other samples showed no significant change after 7 days. The average release rates of the samples with 1000, 500, and 100 ng PDGF-BB during the initial 7 days were 136.98 ± 13, 80.22 ± 6, and 15.62 ± 1 ng/day, respectively. The main release of PDGF-BB occurred early in the experiment because it was not chemically bound to the scaffolds but was physically entrapped during gel formation, and therefore, it diffuses out from the porous hybrid scaffolds. An early release of the chemotactic molecules can be positive for the tissue repairing because it can promote the efficient recruitment of surrounding cells in the damaged tissues. For long-term sustained release of molecules after early cell recruitment, the PCL nanofibers can load proper molecules in purpose. The PCL slowly degrades for years, which is longer than the other synthetic polymers (e.g., poly(lactic acid), poly(glycolic acid)), as well as for chitosan and gelatin [43,44], and the nanofibers exist within the hydrogels in the hybrid scaffolds, and thus, the molecules within the PCL nanofibers will take a longer time to be released.

Examination of hADSC chemotaxis

In the cellular behavior in response to chemical stimulus, chemotaxis is directional movement compared with chemokinesis that is random movement of cells [32]. To assess the hADSC

chemotaxis induced by the released PDGF-BB from the hybrid scaffolds, a stringent migration assay was performed. This is because, in the cell migration assessments, the scratch assay is more useful for observing chemokinesis than chemotaxis, while gravity can also cause cell migration in the Boyden chamber assay besides chemotaxis. In addition, under in vivo conditions, the chemotactic molecules can be active at long distances and diluted by body fluids [31]. Therefore, a stringent migration assay was used to critically evaluate the capacity of the hybrid scaffolds to recruit the hADSCs. As illustrated in Fig. 5a, the hADSCs were grown to confluence on the circular cell culture dishes and partly scrapped, followed by loading the gelated hybrid scaffolds embedded with PDGF-BB on the end point of the scrapped side on the dishes. The hybrid scaffolds containing various amounts of PDGF-BB (1000, 500, and 100 ng PDGF-BB per 1 mL of hybrid scaffolds) and the control group that was without PDGF-BB were used. After a 48 h incubation, the hADSCs were stained with DAPI and examined by a fluorescence microscope, revealing the migration of the hADSCs toward the hybrid scaffolds. The effect of the hADSC chemotaxis was performed under rough conditions which were culturing hADSCs in a serum-free basic medium that suppressed cell proliferation and diluted the released PDGF-BB, and the 2 cm of distance between the hybrid scaffolds and the hADSCs.

Fig. 5b, c shows that the number of hADSCs migrating toward the hybrid scaffolds increased with increasing concentration of PDGF-BB in the hybrid scaffolds, while there was hardly any migration of the hADSCs in the control group. Moreover, the migration beyond the drawn line (green line) was the highest in the 1000 ng PDGF-BB-embedded hybrid scaffolds group. Furthermore, compared with the controls, the migration of the hADSCs was 11.2, 7.8, and 4.6 times more in the 1000, 500, and 100 ng PDGF-BB groups, respectively. Fig. 5d, e shows the difference in migration of the hADSCs among the three divided distances from the front line (green line) of the cell to the scaffold (i.e., start from the green line, 200 μm or less, 200500 μm, and 500 μm or more) according to the PDGF-BB concentration in the hybrid scaffolds. We observe that in all divided distance ranges, the number of migrated hADSCs increases with increasing PDGF-BB concentration (Fig. 5d). We further observe that at distances beyond 500 μm, there are almost no migrated hADSCs in the control group while a large number of migrated hADSCs are seen in the 1000 ng PDGF-BB group. The distribution of the migrated hADSCs at each PDGF-BB concentration is indicated in Fig. 5e. We observe that in the control group, $72.6 \pm 8.9\%$ of the hADSCs migrated less than 200 μm, and only $5.9 \pm 3.5\%$ of the hADSCs migrated beyond 500 μm from the cell front line. On the contrary, in the 500 and 1000 ng PDGF-BB groups, most of the hADSCs migrated beyond 500 μm. Especially in the 1000 ng PDGF-BB group, approximately 50% of the hADSCs migrated beyond 500 μm. These results indicate that our proposed hybrid scaffolds are suitable carriers for PDGF-BB and induce endogenous hADSC recruitment even under the tough conditions of dilution, long distance, and absence of serum.

Conclusion

We fabricated hybrid scaffolds consisting of chitosan/gelatin hydrogel and PCL nanofibers embedded with PDGF-BB for hADSC recruitment. As tissue engineering matrixes, the hybrid scaffolds exhibited cytocompatibility and thermoresponsive characteristics with controllable high modulus after gelation at 37 °C. And the hybrid scaffolds embedded with PDGF-BB had the capability of hADSC chemotaxis. In addition, the PCL nanofibers in the hybrid scaffolds enabled them to have enhanced high modulus and a structure similar to that of native ECM in the cartilage. According to the results of this study, the use of injectable and thermoresponsive hybrid scaffolds is a promising approach as a less invasive tissue engineering strategy for damaged load-bearing cartilage such as IVD. In future studies, in vitro studies of hADSC differentiation to targeted cells (e.g., chondrolcytes) within the hybrid scaffolds and accurate in vivo experiments should be performed focusing on the regeneration of damaged tissues.

Conflicts of interest

The authors declare no competing financial interest.

Acknowledgements

This research was supported by the Bio & Medical Technology Development Program of the National Research Foundation of Korea (NRF) grant funded by the Ministry of Science, ICT and Future Planning and Korea government (MSIT) (No. NRF-2016M3A9B4919711 and NRF-2017M3A9E9073680).

Appendix A. Supplementary data

Supplementary material related to this article can be found, in the online version, at doi:https://doi.org/10.1016/j.jiec.2019.09.046.

References

[1] M. Liu, X. Zeng, C. Ma, H. Yi, Z. Ali, X.B. Mou, S. Li, Y. Deng, N.Y. He, Bone Res. 5 (2017).
[2] A.S. Hoffman, Adv. Drug Deliv. Rev. 64 (2012) 18.
[3] A. Vedadghavami, F. Minooei, M.H. Mohammadi, S. Khetani, A.R. Kolahchi, S. Mashayekhan, A. Sanati-Nezhad, Acta Biomater. 62 (2017) 42.
[4] E. Dashtimoghadam, H. Mirzadeh, F.A. Taromi, B. Nystrom, RSC Adv. 4 (2014) 39386.
[5] C.D. Ji, J. Shi, Mater. Sci. Eng. C Mater. 33 (2013) 3780.
[6] A. Chetouani, N. Follain, S. Marais, C. Rihouey, M. Elkolli, M. Bounekhel, D. Benachour, D. Le Cerf, Int. J. Biol. Macromol. 97 (2017) 348.
[7] A. Sasson, S. Patchornik, R. Eliasy, D. Robinson, R. Haj-Ali, J. Mech. Behav. Biomed. 8 (2012) 143.
[8] S.M. Saraiva, S.P. Miguel, M.P. Ribeiro, P. Coutinho, I.J. Correia, RSC Adv. 5 (2015) 63478.
[9] N.C. Cheng, W.J. Lin, T.Y. Ling, T.H. Young, Acta Biomater. 51 (2017) 258.
[10] C.S. Wang, N. Virgilio, P.M. Wood-Adams, M.C. Heuzey, Food Hydrocoll. 79 (2018) 462.
[11] J.K. Wise, A.L. Yarin, C.M. Megaridis, M. Cho, Tissue Eng. A 15 (2009) 913.
[12] R.Y. Xue, Y.N. Qian, L.H. Li, G.D. Yao, L. Yang, Y.P. Sun, Stem Cell Res. Ther. 8 (2017).
[13] M. Borjigin, B. Strouse, R.A. Niamat, P. Bialk, C. Eskridge, J.W. Xie, E.B. Kmiec, Mol. Ther. Nucl. Acids 1 (2012).
[14] C. Sharma, A.K. Dinda, P.D. Potdar, C.F. Chou, N.C. Mishra, Mater. Sci. Eng. C Mater. Biol. Appl. 64 (2016) 416.
[15] H. Hamedi, S. Moradi, S.M. Hudson, A.E. Tonelli, Carbohydr. Polym. 199 (2018) 445.
[16] I.K. Ko, S.J. Lee, A. Atala, J.J. Yoo, Exp. Mol. Med. 45 (2013).
[17] Y. Yu, R.X. Wu, Y. Yin, F.M. Chen, J. Mater. Chem. B 4 (2016) 569.
[18] E.A. Makris, A.H. Gomoll, K.N. Malizos, J.C. Hu, K.A. Athanasiou, Nat. Rev. Rheumatol. 11 (2015) 21.
[19] W.L. Grayson, B.A. Bunnell, E. Martin, T. Frazier, B.P. Hung, J.M. Gimble, Nat. Rev. Endocrinol. 11 (2015) 140.
[20] K. Tsuruma, M. Yamauchi, S. Sugitani, T. Otsuka, Y. Ohno, Y. Nagahara, Y. Ikegame, M. Shimazawa, S. Yoshimura, T. Iwama, H. Hara, Stem Cell Transl. Med. 3 (2014) 42.
[21] W. Tsuji, J.P. Rubin, K.G. Marra, World J. Stem Cells 6 (2014) 312.
[22] G. Fontana, D. Thomas, E. Collin, A. Pandit, Adv. Healthc. Mater. 3 (2014) 2012.
[23] N. Fani, M. Farokhi, M. Azami, A. Kamali, N.L. Bakhshaiesh, S. Ebrahimi-Barough, J. Ai, M.B. Eslaminejad, ACS Biomater. Sci. Eng. 5 (2019) 2134.
[24] Z.Q. Liu, H.B. Wang, Y. Wang, Q.X. Lin, A.N. Yao, F. Cao, D.X. Li, J. Zhou, C.M. Duan, Z.Y. Du, Y.M. Wang, C.Y. Wang, Biomaterials 33 (2012) 3093.
[25] F.Y. Lai, N. Kakudo, N. Morimoto, S. Taketani, T. Hara, T. Ogawa, K. Kusumoto, Stem Cell Res. Ther. 9 (2018).
[26] Y. Zhao, H. Zhang, Cytotherapy 18 (2016) 816.
[27] Z.W. Xie, C.B. Paras, H. Weng, P. Punnakitikashem, L.C. Su, K. Vu, L.P. Tang, J. Yang, K.T. Nguyen, Acta Biomater. 9 (2013) 9351.
[28] S. Salha, S. Gehmert, V. Brebant, A. Anker, M. Loibl, L. Prantl, S. Gehmert, Clin. Hemorheol. Microcirc. 70 (2018) 543.
[29] B. Wagner, Y. Gorin, Am. J. Physiol. Renal. 306 (2014) F85.
[30] S. Kim, B.H. Shin, C. Yang, S. Jeong, J.H. Shim, M.H. Park, Y.B. Choy, C.Y. Heo, K. Lee, Polym. Basel 10 (2018).
[31] M.C. Phipps, Y.Y. Xu, S.L. Bellis, PLoS One 7 (2012).

[32] D. Yoon, H. Kim, E. Lee, M.H. Park, S. Chung, H. Jeon, C.H. Ahn, K. Lee, Biomater. Res. 20 (2016) 25.
[33] Y.J. Ryu, T.J. Cho, D.S. Lee, J.Y. Choi, J. Cho, Mol. Cells 35 (2013) 557.
[34] J.F. Ge, L. Guo, S. Wang, Y.L. Zhang, T. Cai, R.C.H. Zhao, Y.J. Wu, Stem Cell Rev. Rep. 10 (2014) 295.
[35] J.H. Wang, Q. Yang, N.M. Cheng, X.J. Tao, Z.H. Zhang, X.M. Sun, Q.Q. Zhang, Mater. Sci. Eng. C Mater. 61 (2016) 705.
[36] W.M. Chen, J. Ma, L. Zhu, Y. Morsi, H. El-Hamshary, S.S. Al-Deyab, X.M. Mo, Colloid Surf. B 142 (2016) 165.
[37] J.K. Mouw, G.Q. Ou, V.M. Weaver, Nat. Rev. Mol. Cell Biol. 15 (2014) 771.
[38] X.H. Zhang, M.R. Reagan, D.L. Kaplan, Adv. Drug Deliv. Rev. 61 (2009) 988.
[39] L.T.B. Nguyen, A.O.O. Odeleye, C.Y. Chui, T. Baudequin, Z.F. Cui, H. Ye, Sci. Rep. 9 (2019).
[40] J.V. Araujo, A. Martins, I.B. Leonor, E.D. Pinho, R.L. Reis, N.M. Neves, J. Biomater. Sci. Polym. E 19 (2008) 1261.
[41] E.A. Growney Kalaf, M. Pendyala, J.G. Bledsoe, S.A. Sell, J. Mech. Behav. Biomed. Mater. 72 (2017) 229.
[42] M. Recuerda, D. Perie, G. Gilbert, G. Beaudoin, BMC Musculoskelet Disord. 13 (2012) 195.
[43] I. Armentano, M. Dottori, E. Fortunati, S. Mattioli, J.M. Kenny, Polym. Degrad. Stabil. 95 (2010) 2126.
[44] H.F. Sun, L. Mei, C.X. Song, X.M. Cui, P.Y. Wang, Biomaterials 27 (2006) 1735.